(ρ) and the fact that the correlation is better by using σ^+ values rather than σ values, it has been suggested[29] that hydrogen abstraction by *t*-BuO· occurs through an electrophilic mechanism; i.e., partial charge separation takes place in the transition state. However, more recent studies[5,30] under conditions where complications due to chain reactions from chlorine atoms are eliminated gave much lower values for ρ (−0.32 to −0.39) for the reactions of *t*-BuO· with para-substituted toluenes. It has been claimed[5] that ρ reflects the differences in the bond dissociation energies of substituted toluenes (rather than the electrophilic nature of the abstraction mechanism) and that its magnitude is a measure of the sensitivity of the abstracting radical to these differences. Our data with substituted phenols clearly give a ρ of significantly larger magnitude, and the plot of log k_3 against σ^+ gives a linear fit with better correlation than the plot of log k_3 against σ. This, coupled with the fact that phenol as a substrate is more susceptible to polar effects in the transition state than toluene, suggests that the reaction of *t*-BuO· with phenols would probably be best understood by an approach based on partial charge separation in the transition state (i.e., electrophilic mechanism).

We attempted to observe electron-transfer reaction, if any, between *t*-BuO· and *p*-dimethoxybenzene. The experiments were carried out in systems where benzene, *tert*-butyl alcohol, and a mixture (1:1) of *tert*-butyl alcohol and acetic acid were used as cosolvent with di-*tert*-butyl peroxide. There was no indication of the formation of cation of dimethoxybenzene in the spectral region 440–480 nm[31] nor was there any significant difference in the rate of formation of diphenylhydroxymethyl radical from diphenylmethanol in the presence and absence of *p*-dimethoxybenzene. Evidently, *t*-BuO· does not interact with *p*-dimethoxybenzene either by electron transfer or by any other mechanism (e.g., attack at the phenyl ring) under the conditions of our experiments.

In view of the fact[11-13] that carbonyl triplets present many similarities with *t*-BuO· in their hydrogen abstraction reactions, it is of interest to compare the kinetics of *t*-BuO· and benzophenone triplet in respect of their reactions with phenols. The data for benzophenone triplet are presented in the preceding paper. Both *t*-BuO· and benzophenone triplet appear to abstract hydrogen from phenols faster than from other substrates (e.g., hydrocarbons, alcohols, and ethers).[7,11] For a particular phenol, the rate constant for hydrogen abstraction by *tert*-butoxy radicals (in 1:2 benzene–di-*tert*-butyl peroxide) is smaller than the rate constant for the quenching of benzophenone triplets in benzene. The difference may reflect the increased importance of polar effects in the case of the benzophenone triplets while, in the case of *tert*-butoxy, the reactivity is largely (but not only?) controlled by the bond energy at the ArO–H site. While the Hammett ρ values may not seem to favor this argument, we note that bond energies are somewhat sensitive to substituent effects and also that in the case of benzophenone, the faster reaction tends to decrease the sensitivity of the process to changes in the substrates.

It is clear that while in the case of *tert*-butoxy radicals the only reaction is hydrogen transfer, in the case of benzophenone triplets other interactions can also play a significant role; for example, the yields are low where a heavy atom is present in the substrate, as well as in experiments at low temperatures.[32] Thus, in terms of overall mechanism, the case of benzophenone triplets appears to be more involved than the case of *tert*-butoxy radicals, although the initial interactions of the two systems may be similar. While solvent and Arrhenius parameters for benzophenone triplets and *tert*-butoxy radicals are similar, isotope effects are substantially smaller in the case of benzophenone. This may be directly connected to the increase in rate constants. The behavior of *p*-methoxypropiophenone triplets shows high isotope effects; this is surprising in view of the fact that π,π^* triplets do not usually show radical-like properties.

Experimental Section

Di-*tert*-butyl peroxide was obtained from MC & B; it was distilled and treated in an alumina column before use. Samples prepd. from di-*tert*-butyl peroxide that was only passed through alumina (with no prior distillation) gave essentially the same results. The source and purification of phenols and other chemicals are described in the preceding paper.[32] Diphenylmethanol (MC & B) was sublimed twice before use.

The details of the laser photolysis setup are also given in the preceding paper.[32] All the samples were deaerated by passing oxygen-free argon. In the experiments where the ratio of di-*tert*-butyl peroxide and cosolvent was 2:1, the laser output (~3 mJ) was attenuated to about half its original value by using neutral density filters in order to avoid second-order contributions to the decay of *tert*-butoxy radicals.

(31) The cation of *p*-dimethoxybenzene has on absorption maximum at 460 nm, as shown by pulse radiolytic studies in aqueous solution; O'Neill, P.; Steenken, S.; Schulte-Frohlinde, D. *J. Phys. Chem.* **1975**, *79*, 2773-9.

(32) Das, P. K.; Encinas, M. V.; Scaiano, J. C., preceding paper in this issue.

Reactions of Coordinated Molecules. 30. Carbon–Carbon Bond Formation between Adjacent Acyl Ligands: Transannular Coupling across a Metalla-β-diketonate Ring

C. M. Lukehart* and K. Srinivasan

Contribution from the Department of Chemistry, Vanderbilt University, Nashville, Tennessee 37235. *Received January 19, 1981*

Abstract: When the metalla-β-diketonate complex $[\eta\text{-}C_5H_5(OC)Fe(CH_3CO)(i\text{-}C_3H_7CO)]BF_2$ is treated with a stoichiometric amount of KH, a proton of the acetyl group is removed, affording an anionic complex in essentially quantitative yield with the molecular formula $\{[\eta\text{-}C_5H_5(OC)Fe(CH_2CO)(i\text{-}C_3H_7CO)]BF_2\}^-$. An X-ray structure of the Me_4N^+ salt of this complex is reported: $P2_1/c$ with a = 9.640 (5) Å, b = 14.687 (3), c = 13.277 (3) Å, β = 90.24 (3)°, V = 1880 Å^3, and Z = 4. The molecular structure reveals C–C bond formation between the original acyl carbon atoms. These two carbon atoms and the exomethylene carbon atom adopt an η-allyl coordination to the η-$C_5H_5(OC)Fe$ moiety. This interligand C–C bond formation represents a transannular coupling across the six-membered metalla-β-diketonate ring. The significance of this result pertaining to stoichiometric and catalytic reaction chemistry at metal atoms is discussed.

We reported recently the synthesis of several (metalla-β-diketonato) BXY complexes,[1,2] and an X-ray structure of one such ferra complex, $[\eta\text{-}C_5H_5(OC)Fe(CH_3CO)(i\text{-}C_3H_7CO)]BF_2$, **1**.[3] In complex **1**, the boron atom acts as a central coordinating atom

0002-7863/81/1503-4166$01.25/0

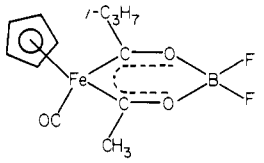

1

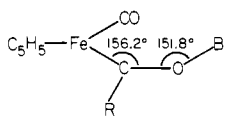

2

where the BF_2 group is bonded to the two acyl oxygen atoms, forming a six-membered, ferra-β-diketonate ring. This ferra-β-diketonate ring adopts a boat-shaped conformation, as shown in **2**. As discussed earlier, a boat-shaped conformation for a metalla-β-diketonate ring arises presumably from relief of angle strain within the chelate ring.[3]

As part of our continuing study of the chemistry of metalla-β-diketonate compounds, we decided to prepare metalla derivatives of the α-anions of β-diketones and explore the chemistry of these species. The simplest organic analogue to these complexes is the dianionic form of acetylacetone where the enolic proton and one of the methyl group protons have been removed.

Considerable spectroscopic evidence indicated that (metalla-β-diketonato)BX_2 complexes have relatively electron-poor, metalla-chelate rings due to the high electronegativity of the boron dihalide group. These complexes should best stabilize an α-anion, if formed, and would, therefore, have relatively acidic hydrogen atoms on the carbon atoms attached to the metalla-chelate ring. These protons should also be quite acidic because of the partial carbenoid character of the metal–ligand bonding within a metalla-β-diketonate ring.[4,5]

We chose to form the conjugate base of complex **1** because (1) complex **1** is the most well-characterized (metalla-β-diketonato)BF_2 complex and (2) the kinetic deprotonation of the acetyl methyl protons is sufficiently greater than that of the isopropyl methine proton so that only a monoanion would be formed. When complex **1** is treated with a stoichiometric amount of KH in THF solution at 25 °C, an essentially quantitative conversion of **1** to its monoanion occurs concomitant with the evolution of hydrogen gas. Quite unexpectedly, this anion could not be protonated, deuterated, or alkylated successfully.

An X-ray structure of the anion reveals that interlignad, carbon–carbon bond formation has occurred between the original acyl carbon atoms. This transannular C–C coupling converts the six-membered ferra-β-diketonate ring into a formal 3:5 bicyclic system. The coupled carbon atoms and the exomethylene carbon atom generated from deprotonation of the original acetyl methyl group bond to the Fe moiety as a η-allylic ligand. We believe that this C–C bond formation at a mononuclear site has considerable significance in the stoichiometric and catalytic chemistry which may occur in organometallic complexes. In this report, we attempt to rationalize the observed chemistry and to generalize the significance of this transformation.

Experimental Section

All reactions and other manipulations were performed under dry, prepurified nitrogen. Tetrahydrofuran (THF) and diethyl ether were dried over Na/K alloy with added benzophenone, and methylene chloride and acetone-d_6 were dried over P_2O_5.

Infrared spectra were recorded on a Perkin-Elmer 727 spectrometer as methylene chloride solutions in 0.10-mm sodium chloride cavity cells with the solvent as a reference and a polystyrene film as a calibration standard. ^1H NMR spectra were obtained on a JOEL MH-100 NMR spectrometer as acetone-d_6 solutions with Me_4Si as an internal reference. ^{13}C NMR spectra were recorded on a JOEL FX90Q Fourier transform NMR spectrometer operating at a frequency of 22.50 MHz as acetone-d_6 solutions at 36 °C. The ^2H signal of the solvent was used for locking and a pulse width of 10 μs was used. A repetition rate of 2.3 s was employed to collect ca. 9000 pulses/spectrum. Preliminary spectra were proton decoupled, using a 1000-Hz bandwidth. Peak assignments and exact C–H coupling constants were obtained using gated decoupling. Samples consisted of ~35 mg of complex and ~0.5 mg of $Cr(acac)_3$ dissolved in ~0.4 mL of solvent with Me_4Si as an internal reference. Microanalysis was performed by Galbraith Laboratories, Inc., Knoxville, Tn.

The complex η-$C_5H_5(OC)_2FeC(O)CH(CH_3)_2$, **3**, was prepared by a literature method,[6] and complex **1** was prepared by a slight modification of a known procedure.[2]

Preparation of $[\eta$-$C_5H_5(OC)Fe(CH_3CO)(i$-$C_3H_7CO)]BF_2$ (1). To a stirred solution of 2.39 g (9.6 mmol) of **3** in 130 mL of ether at −50 °C was added dropwise 6.86 mL of a 1.4 M solution of methyl lithium in ether over a 5-min period. After stirring the solution at −50 °C for 30 min, the solvent was removed at −10 °C at reduced pressure. The reaction residue was suspended in 120 mL of CH_2Cl_2 and was cooled to −78 °C. Gaseous BF_3 was bubbled through this suspension at a moderate rate for 4 min. After stirring the reaction mixture at −78 °C for an additional 30 min and at 0 °C for 90 min, the solvent and excess BF_3 were removed at reduced pressure. The reaction residue was extracted with toluene. The extract was filtered, and removal of the toluene at reduced pressure gave the crude product. Crystallization from ether solution at −20 °C afforded 1.40 g (49%) of **1** as yellow crystals.

Preparation of $Me_4N[[\eta$-$C_5H_5(CO)Fe(CH_2CO)(i$-$C_3H_7CO)]BF_2]$ (4). To a stirred suspension of 0.13 g (3.2 mmol) of KH in 50 mL of THF was added 0.93 g (3.0 mmol) of **1** at 25 °C. The yellow reaction solution turned red immediately after this addition, and this color change was accompanied by brisk evolution of hydrogen. The solution was stirred for 20 min, and then the solvent was removed at reduced pressure. To the solid residue was added 5 mL of a saturated solution of Me_4NCl in degassed water and 40 mL of CH_2Cl_2; the mixture was stirred for 30 min. The CH_2Cl_2 layer was dried over 4 Å molecular sieves. Removal of the solvent gave the crude product. Crystallization from THF/ether solution at −20 °C afforded 0.40 g (32%) of **4** as red monoclinic crystals; 138–144 °C dec: IR ν (CO) 1895 (broad); ^1H NMR δ 0.448 (heptet, 1, CH, J = 6Hz), 0.457 (d, 1, CH_2 (*anti*-**H**), J = 3.5 Hz), 0.99 (d, 3, CH_3, J = 6 Hz), 1.40 (d, 3, CH_3, J = 6 Hz), 3.00 (d, 1, CH_2 (*syn*-H), J = 3.5 Hz), 3.46 (s, 12, NCH_3), 4.31 (s, 5, C_5H_5); ^{13}C NMR δ 16.7 (t, CH_2, J = 154 Hz), 22.6 (q, CH_3, J = 125 Hz), 23.6 (q, CH_3, J = 124 Hz), 38.4 (d, CH, J = 127 Hz), 56.0 (q of t, NCH_3, J_{CH} = 144 Hz, J_{CN} = 4 Hz(t)), 82.2 (d of t, C_5H_5, J_{CH_α} = 177 Hz, J_{CH_β} = 7 Hz), 113.5 (s, C), 122.5 (s, C), 223.0 (s, CO). Anal. ($C_{16}H_{26}NO_3BFeF_2$) C, H, F.

X-ray Crystallography. Red crystals of **4** were obtained as described above. Collection of the X-ray data and the Lorentz, polarization, and empirical absorption corrections were performed by Molecular Structure Corporation, College Station, TX, as a commercial, technical service.

A monoclinic crystal of dimensions 0.35 × 0.35 × 0.35 mm was mounted in a glass capillary. Preliminary examination of the crystal on the diffractometer showed monoclinic symmetry. The systematic absences indicated the space group $P2_1/c$. Cell constants at 23 ± 1 °C obtained from the computer centering of 24 reflections were: a = 9.640 (5) Å, b = 14.687 (3) Å, c = 13.277 (3) Å, β = 90.24 (3)°, V = 1879.9 Å^3, d(calcd) = 1.322 g/cm^3 with Z = 4.

For specific details of data collection and data reduction see the Supplementary Material Available paragraph. The data were collected on an Enraf-Nonius CAD4 diffractometer using Mo K_α (λ = 0.71073 Å) radiation and a graphite crystal incident beam monochrometer. A total of 3579 reflections in the range $0° < 2\theta < 50°$ were collected, of which 2729 were unique and were used to solve and refine the structure. No crystal decomposition during data collection was observed. The relative intensity varied from 99.7% to 85.9% with an average of 92.1% on I.

Solution and refinement followed a previously published method.[3] A sharpened Patterson function revealed the Fe position and provided phases for a difference synthesis to locate the remaining atoms. All nonhydrogen atoms were located and refined anisotropically. All hydrogen atoms of the anionic Fe complex were located and refined isotropically, while all hydrogen atoms of the Me_4N cation were located and included in the calculations but were not refined. The final R factor was 0.070, and the weighted R factor was 0.063, both calculated with all 2729 unique reflections. The maximum shift-to-error ratio for the atomic parameters in the final cycle was 0.147. The maximum electron density on the final difference map was 0.69 e/Å^3 located 1.0 Å from Fe. A table of atomic positional and thermal parameters and a listing of observed and calculated structure factors are provided as supplementary material.

Results and Discussion

When a THF solution of the ferra-β-diketonate complex **1** is treated with a stoichiometric amount of KH at 25 °C, a brisk

(1) Lukehart, C. M.; Warfield, L. T. *Inorg. Chem.* **1978**, *17*, 201.
(2) Lukehart, C. M.; Warfield, L. T. *J. Organometal. Chem.* **1980**, *187*, 9.
(3) Lenhert, P. G.; Lukehart, C. M.; Warfield, L. T. *Inorg. Chem.* **1980**, *19*, 2343.
(4) Lukehart, C. M.; Torrence, G. P.; Zeile, J. V. *J. Am. Chem. Soc.* **1975**, *97*, 6903.
(5) Casey, C. P.; Anderson, R. L. *J. Am. Chem. Soc.* **1974**, *96*, 1230.
(6) Lukehart, C. M.; Zeile, J. V. *J. Am. Chem. Soc.* **1977**, *99*, 4368.

Table I. Selected Interatomic Distances (in Å, with Esd's) for $\{[\eta\text{-}C_5H_5(OC)Fe(CH_2CO)(i\text{-}C_3H_7CO)]BF_2\}^-$

atoms	distance	atoms	distance
Fe-C(1)	2.085 (5)	B-F(2)	1.401 (5)
Fe-C(2)	2.095 (4)	C(10)-C(11)	1.410 (7)
Fe-C(3)	2.186 (4)	C(11)-C(12)	1.398 (7)
Fe-C(7)	1.718 (5)	C(12)-C(13)	1.402 (7)
Fe-C(10)	2.089 (5)	C(13)-C(14)	1.416 (7)
Fe-C(11)	2.088 (5)	C(14)-C(10)	1.399 (7)
Fe-C(12)	2.098 (5)	C(1)-H(1)	1.00 (5)
Fe-C(13)	2.092 (5)	C(1)-H(2)	0.86 (5)
Fe-C(14)	2.096 (5)	C(4)-H(4)	1.01 (4)
C(7)-O(7)	1.171 (6)	C(10)-H(10)	0.87 (4)
C(1)-C(2)	1.397 (6)	C(11)-H(11)	0.88 (5)
C(2)-C(3)	1.410 (6)	C(12)-H(12)	0.93 (4)
C(3)-C(4)	1.522 (6)	C(13)-H(13)	0.91 (5)
C(4)-C(5)	1.540 (9)	C(14)-H(14)	0.94 (4)
C(4)-C(6)	1.510 (8)	C(5)-H(51)	0.98 (6)
C(2)-O(2)	1.370 (5)	C(5)-H(52)	1.16 (7)
C(3)-O(3)	1.393 (5)	C(5)-H(53)	0.81 (7)
O(2)-B	1.464 (6)	C(6)-H(61)	0.84 (7)
O(3)-B	1.459 (5)	C(6)-H(62)	0.98 (9)
B-F(1)	1.407 (5)	C(6)-H(63)	0.95 (6)

evolution of hydrogen is observed as the reaction solution changes from yellow to red. Metathetical exchange of K^+ for Me_4N^+ affords red crystals of **4** upon crystallization. Compound **4** is

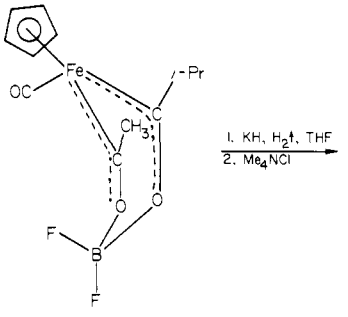

1

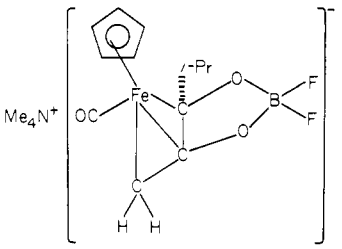

4

ionic based on its solubility properties. The observed ca. 100 cm^{-1} ν (CO) shift to lower energy when **1** is converted to **4** also indicates that the iron complex is anionic.

Although **4** is the stoichiometric conjugated base of **1**, it is quite different structurally. Protonation, deuteration, or alkylation of the K^+ analogue of **4** did not afford **1** or its deuterated or alkylated derivatives. Crystallographic analysis of **4** revealed that the adjacent acyl carbons of **1** underwent transannular coupling. These former acyl carbon atoms and the exocyclic methylene carbon atom coordinate to the iron atom as a highly substituted η-allylic ligand. An ORTEP view of the anionic part of **4** is shown in Figure 1, and selected interatomic distances and angles are compiled in Tables I and II, respectively. Selected least-squares plane data are listed in Table III.

The $(\eta\text{-}C_5H_5)Fe(CO)$ moiety along with C(1) and C(3) form a slightly distorted "three-legged piano stool" structure where the angles C(7)–Fe–C(1), C(7)–Fe–C(3) and C(1)–Fe–C(3) are 89.6 (2)°, 93.6 (2)°, and 71.1 (2)°, respectively. Carbon–carbon distances within the C_5H_5 ring range from 1.398 (7) to 1.416 (7) Å with an average value of 1.405 (7) Å. The C_5H_5–Fe distance of 1.718 Å is only 0.04 Å shorter than that distance in **1**.[3] The Fe–C(7) distance of 1.718 (5) Å is 0.031 Å shorter than the corresponding distance in **1**, which may reflect a greater negative charge density on the Fe atom of **4**.

Table II. Selected Bond Angles (in Deg, with Esd's) for $\{[\eta\text{-}C_5H_5(OC)Fe(CH_2CO)(i\text{-}C_3H_7CO)]BF_2\}^-$

atoms	angle	atoms	angle
C(1)-Fe-C(2)	39.1 (2)	C(2)-O(2)-B	107.2 (3)
C(2)-Fe-C(3)	38.4 (2)	C(3)-O(3)-B	108.0 (3)
C(1)-Fe-C(7)	89.6 (2)	O(2)-B-O(3)	105.8 (4)
C(3)-Fe-C(7)	93.6 (2)	O(2)-B-F(1)	110.5 (4)
Fe-C(7)-O(7)	174.3 (5)	O(2)-B-F(2)	111.6 (4)
Fe-C(1)-C(2)	70.9 (3)	O(3)-B-F(1)	111.1 (4)
Fe-C(2)-C(3)	74.3 (3)	O(3)-B-F(2)	111.9 (4)
Fe-C(3)-C(4)	115.2 (3)	F(1)-B-F(2)	106.1 (4)
Fe-C(2)-O(2)	118.5 (3)	C(10)-C(11)-C(12)	108.1 (5)
Fe-C(3)-O(3)	120.2 (3)	C(11)-C(12)-C(13)	107.8 (5)
C(1)-C(2)-C(3)	124.5 (4)	C(12)-C(13)-C(14)	108.5 (5)
C(2)-C(3)-C(4)	125.6 (4)	C(13)-C(14)-C(10)	107.1 (5)
C(3)-C(4)-C(5)	109.2 (5)	C(14)-C(10)-C(11)	108.5 (5)
C(3)-C(4)-C(6)	111.9 (5)	C(2)-C(1)-H(1)	114 (3)
C(5)-C(4)-C(6)	112.4 (5)	C(2)-C(1)-H(2)	117 (4)
C(1)-C(2)-O(2)	123.2 (4)	H(1)-C(1)-H(2)	114 (4)
C(4)-C(3)-O(3)	113.5 (4)	C(3)-C(4)-H(4)	106 (3)
C(2)-C(3)-O(3)	108.1 (4)	C(5)-C(4)-H(4)	104 (3)
C(3)-C(2)-O(2)	110.9 (4)	C(6)-C(4)-H(4)	112 (3)

Table III. Selected Least-Squares Planes[a] and Atomic Deviations from the Planes for $\{[\eta\text{-}C_5H_5(OC)Fe(CH_2CO)(i\text{-}C_3H_7CO)]BF_2\}^-$

atoms[b]	dev, Å	atoms	dev, Å
Plane I: $-0.28363I + 0.65908J - 0.69654K = -0.68239$			
C(10)	0.0024	Fe	−1.718
C(11)	−0.0023		
C(12)	0.0013		
C(13)	0.0002		
C(14)	−0.0016		
Plane II: $-0.45135I + 0.55530J - 0.69852K = -4.4399$			
C(1)	0	Fe	1.579
C(2)	0	O(2)	0.297
C(3)	0	O(3)	0.288
		C(4)	−1.001
Plane III: $0.53784I + 0.77899J - 0.32234K = 0.56412$			
Fe	0	C(2)	0.596
C(1)	0		
C(3)	0		
Plane IV: $0.62286I - 0.48505J + 0.61381K = 5.3192$			
C(2)	0.0124	F(1)	1.204
C(3)	0.0045	F(2)	−1.035
O(2)	−0.0232	C(1)	−0.217
O(3)	−0.0186	C(4)	0.832
B	0.0249	Fe	−1.792
Plane V: $-0.41758I - 0.55548J + 0.71908K = -1.0869$			
Fe	0	C(1)	0.903
C(2)	0	C(4)	1.192
C(3)	0	O(2)	−1.159
		O(3)	−1.191
Plane VI: $0.64031I - 0.47626J + 0.60264K = 5.4136$			
C(2)	0.0042	B	0.066
C(3)	−0.0041	C(1)	−0.250
O(2)	−0.0025	C(4)	0.803
O(3)	0.0025		
Plane VII: $-0.010456I + 0.78250J + 0.62257K = -3.1371$			
B	0	Fe	0.189
F(1)	0	C(1)	1.536
F(2)	0	C(2)	0.717
		C(3)	−0.694
		C(7)	−0.417
		O(7)	−0.781

[a] Equations of the planes are expressed as $PI + QJ + RK = S$ in orthogonal angstrom space (see text for angles of intersecting planes). [b] Atoms used in calculating planes.

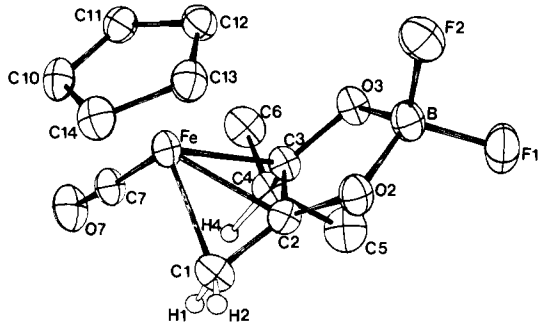

Figure 1. An ORTEP view of $\{[\eta\text{-}C_5H_5(OC)Fe(CH_2CO)(i\text{-}C_3H_7CO)]\text{-}BF_2\}^-$ showing the atomic numbering scheme (ellipsoids at 30%). Although all H atoms were located and refined, most are not shown for clarity.

The Fe–C(1), –C(2), and –C(3) distances of 2.085 (5), 2.095 (4), and 2.186 (4) Å, respectively, represent normal Fe–C distances to η-allylic ligands. Although the Fe–C(3) distance is only slightly, but significantly, longer than the other two Fe–C distances, the Fe–C(1) and Fe–C(2) distances are not significantly different. In the isoelectronic $(\eta\text{-}C_3H_5)Fe(CO)_3X$ complexes (where X is Br or the same organometallic fragment), Fe–C distances to the outer allylic carbon atoms range from 2.126 (8) to 2.208 (4) Å, and Fe–C distances to the inner carbon atoms are 2.058 (11) and 2.104 (4) Å.[7] Within a series of substituted η-allyl complexes of the type $(\eta\text{-allyl})Fe(CO)_3R$ whose structures have been well-determined, the two Fe–C (outer) and Fe–C (inner) distances range from 2.117 (8) to 2.163 (7) Å or 2.140 (4) to 2.173 (8) Å and 2.060 (14) to 2.094 (8) Å, respectively.[8] These complexes are also isoelectronic to **4**. More detailed structural comparisons are not warranted due to the unusual substitution on the allylic ligand of **4**.

In **4**, the allylic C(1)–C(2) and C(2)–C(3) distances of 1.397 (6) and 1.410 (6) Å, respectively, and the C(1)–C(2)–C(3) angle of 124.5 (4)° are not significantly different from the corresponding distances and angles determined for the η-allyl ligands of the isoelectronic complexes mentioned above.[7,8] The Fe atom is 1.579 Å from the [C(1), C(2), C(3)] plane, and the dihedral angle between this plane and the [Fe, C(1), C(3)] plane is 65.5°, which is consistent with η-allyl coordination. The C(3)–C(4), C(4)–C(5), and C(4)–C(6) distances represent normal single bond distances. The C(4)–C(3)–O(3) angle of 113.5 (4)° reveals a deviation from sp^2 hybridization at C(3).

The two intraligand C–O distances [average value of 1.382 (5) Å] are essentially equal within $\pm 2.5\sigma$. However, this average distance is 0.088 (5) Å longer than the corresponding average acyl C–O distance in **1** and is nearly as long as the C–O distance in dimethyl ether [1.416 (5) Å].[9] This C–O bond lengthening in **4** compared to **1** reflects a change in hybridization at C(2) and C(3) toward greater p character.

The boron coordination geometry is nearly tetrahedral with normal B–O and B–F distances. The boron atom completes an unusual five-membered ring, O(2)–C(2)–C(3)–O(3)–B, which incorporates two of the allylic carbon atoms. This ring is essentially planar, plane IV (maximum atomic deviation is 0.025 Å), and it intersects the [Fe, C(2), C(3)] plane with a dihedral angle of 63.2°. The atoms C(2), O(2), C(3), and O(3) form a slightly better plane (maximum atomic deviation is 0.004 Å); the boron atom lies 0.066 Å below this plane. Plane IV intersects the [C(1), C(2), C(3)] plane with a dihedral angle of only 11.7°. The O(2)···O(3) "bite" distance of 2.331 (4) Å is 0.091 Å shorter than the corresponding "bite" distance in **1**, which presumably results from the smaller O(2)–B–O(3) angle in **4** due to the planar five-membered ring formation. The internal angles within this C_2O_2B ring range from 105.8 to 110.9° and give a sum of 540.0°.

The Me_4N^+ ion is tetrahedral with an average N–C distance of 1.478(7) Å. The Fe···N distance is 5.41 Å.

The NMR data are consistent with the above structural description of **4**. ^1H NMR spectral comparisons between **4**, **1**[2] and the neutral $\eta\text{-}C_5H_5(OC)Fe(\eta\text{-}C_3H_5)$[10] complex are particularly informative. The proton spectrum of **4** compared to that of **1** reveals (1) an upfield shift of ~0.7 ppm for the C_5H_5 resonance of **4** due presumably to greater electron density on the Fe atom, (2) an anisochronism of 41 Hz for the isopropyl methyl groups of **4** due to the greater asymmetry of **4**,[11] (3) an upfield shift of 3.26 ppm for the methine proton resonance of **4** because C(3) has lost its acylic character, and (4) a Me_4N^+ resonance at δ 3.46.

As expected, the methylene protons of **4**, H(1) and H(2), have allylic rather than acylic chemical shifts of δ 0.457 and 3.00, respectively, corresponding to anti and syn protons on a terminal carbon atom of an η-allylic ligand. In $\eta\text{-}C_5H_5(OC)Fe(\eta\text{-}C_3H_5)$, the anti and syn proton resonances appear at δ 0.68 and 2.67, respectively, in benzene solution. A geminal H(1)–H(2) coupling constant of ~3.5 Hz is observed in **4** also.

The ^{13}C NMR resonances of C(4), C(5), C(6), C(7), and C(10)–C(14) have normal chemical shifts for these carbon environments.[12-15] Unfortunately, unambiguous assignment of the allylic quarternary carbon resonances is not possible because of the absence of ^{13}C NMR data for a suitable model complex. The C(1) resonance appears at δ 16.7 with a J_{CH} coupling constant of 154 Hz. Presumably, this relatively high-field chemical shift reflects the increased amount of negative charge on the complex, and the magnitude of the C–H coupling indicates η-allylic hybridization at C(1).[16] The unassigned C(2) and C(3) resonances appear at δ 113.5 and 122.5. These chemical shifts, which are in the η-allylic region, are greatly different from those of acyl carbon atoms in metalla-β-diketonate complexes.[14] The acyl carbon resonances of **1** appear at δ 330.5 and 337.9.[17]

The minimum structural rearrangement required for converting **1** to **4** can be visualized easily. The observed geometry is attained by isomerizing **1** (as shown) to its other boat form, followed by the removal of a proton from the methyl substituent. This geometrical isomerism of **1** has been observed in solution. Alternatively, the mirror image of **1** could be deprotonated followed by a 180° degree rotation of the $\eta\text{-}C_5H_5(OC)Fe$ moiety relative to the rest of the complex.

Upon formation of the η-allylic ligand, the C_2O_2B ring would become planar. The two principal structural changes are (1) the acyl carbon–acyl carbon distance of 2.633 (2) Å in **1** shortens to 1.410 (6) Å when the C(2)–C(3) bond is formed and (2) the Fe···CH_3 contact distance of 3.005 (2) Å in **1** shortens to 2.085 (5) Å when the Fe–C(1) bond is formed.

The electronic rearrangement required to derive **4** from the initial conjugate base form of **1** is of major importance to our understanding of this C–C bond formation. For brevity, we will not discuss equivalent resonance forms. Also, the ferra moiety is required to obey the EAN rule in each structure presented below.

One of the acyl-carbenoid resonance forms of **1**, shown as **5**, is equivalent to Lewis structure **6**. Deprotonation of **6** affords its conjugate base **7**, which should be stabilized as the (σ-vinyl)(carbenoid) complex, **8**. With the negative charge formally on boron and with two π donors attached to C(2), π-electron

(7) Simon, F. E.; Lauher, J. W. *Inorg. Chem.* **1980**, *19*, 2338.
(8) Cotton, F. A.; Frenz, B. A.; Troup, J. M. *J. Organometal. Chem.* **1973**, *61*, 337.
(9) "Tables of Interatomic Distances;" The Chemical Society: London, 1965; Special Publication No. 18.
(10) Green, M. L. H.; Nagy, P. L. I. *J. Chem. Soc.* **1963**, 189.
(11) The anisochronism of the isopropyl methyl groups of **1** was too small to be detected (see ref 2). However, this asymmetry is revealed in the ^{13}C NMR spectrum of **1** (see ref 17).
(12) Mann, B. E. *Adv. Organometal. Chem.* **1974**, *12*, 135.
(13) Gansow, O. A.; Vernon, W. D. "Topics Carbon-13 NMR Spectroscopy"; Levy, G. C. Ed.; Wiley-Interscience: New York, 1976; Vol. 2, Chapter 5.
(14) Darst, K. P.; Lukehart, C. M. *Inorg. Chim. Acta* **1978**, *161*, 1.
(15) Darst, K. P.; Lukehart, C. M. *Inorg. Chim. Acta* **1980**, *41*, 239.
(16) Mann, B. E.; Pietropaolo, R.; Shaw, B. L. *J. Chem. Soc., Dalton Trans.* **1973**, 2390.
(17) ^{13}C NMR data for **1** in acetone-d_6 solution are δ 18.4 (q, $HCCH_3$, J = 127 Hz), 19.7 (q, $HCCH_3$, J = 127 Hz), 49.5 (q, CCH_3, J = 125 Hz), 59.4 (d, CH, J = 136 Hz), 90.5 (d, C_5H_5, J = 178 Hz), 214.4 (s, CO), 330.5 (s, CCH_3), 337.9 (s, C-*i*-Pr).

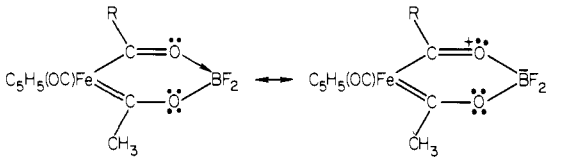

5 6

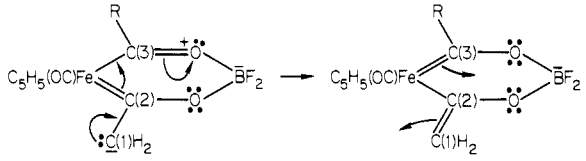

7 8

polarization within the exomethylene bond would make C(1) more negative than C(2). Complex **8** could rearrange as shown to give **9**, which is the all σ representation of the η-allylic structure of **4**.

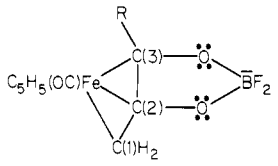

9

Interligand C–C coupling would then occur formally by oxidation of the iron atom when the C(2)–C(3) bond is formed, followed by formation of the Fe–C(1) bond, thus, reducing the Fe atom to its original oxidation state and oxidizing the negatively charged C(1) to a neutral methylene group. By using similar reasoning, it is possible to go directly from **7** to **9**. Both mechanisms can be represented as an electrophilic attack by a positively charged acyl carbon atom on the π-electron pair of an adjacent metal–carbon multiple bond with concomitant reduction of the iron atom.

Clearly, the η-allylic ligand formation in **4** stabilizes this anion sufficiently to permit its isolation. However, we believe that this interligand coupling reaction is important to both stoichiometric and catalytic reaction chemistry at metal atoms. We propose that interligand C–C coupling may occur between adjacent ligands when (1) the two carbon donor atoms have some degree of unsaturation or acylic character, (2) the two carbon atoms are in close contact (the chelate ring of **1** imposes a C(2)···C(3) contact distance of 2.633 (2) Å, which is considerably shorter than an estimated C···C atomic van der Waals contact distance of 3.2 Å), and (3) the metal atom to which these carbon atoms are bonded can be reduced from an external source (such as C(1) in this example). Other electron sources may be available in metal clusters or other types of mononuclear or polynuclear complexes.

Conversion of **1** to **4** also shows that unsaturated ligands may couple *prior to* a reductive-elimination step. Oxidation or reduction of **4** may cleave the Fe–C allylic bonds to afford acyloin or glycol derivatives. Hydrolysis of the BF_2 group and any further reduction should give a glycol product. It should also be noted that C(2) and O(2) were obtained from CO, while the formal derivation of C(3) and O(3) from CO is possible. From this perspective, this coupling reaction represents a C(1) to C(2) hydrocarbon transformation. We are currently examining the generality of such interligand coupling reactions and the reaction chemistry of **4** and its derivatives, including the potential use of this reaction for stereospecific glycol formation.

Acknowledgment. C.M.L. thanks the National Science Foundation (Grant No. CHE-7907557) and the University Research Council of Vanderbilt University for support of this research. C.M.L. acknowledges support from the Alfred P. Sloan Foundation as a Research Fellow. We thank Andrew J. Baskar for technical assistance.

Supplementary Material Available: Details of data collection and data reduction and tables listing the atomic positional and thermal parameters and the observed and calculated structure factors (21 pages). Odering information is given on any current masthead page.

Photolysis of Organopolysilanes. Reaction of Trimethylsilylphenylsilylene with Functional-Group-Substituted Olefins

Mitsuo Ishikawa,* Ken-ichi Nakagawa, Seiji Katayama, and Makoto Kumada*

Contribution from the Department of Synthetic Chemistry, Faculty of Engineering, Kyoto University, Kyoto 606, Japan. *Received June 6, 1980*

Abstract: The photolysis of tris(trimethylsilyl)phenylsilane (**1**) in the presence of vinyl chloride or 1-bromo-2-methylpropene afforded, probably via silacyclopropane intermediates, the respective 1-alkenyl-1-halo-1-phenyltrimethyldisilanes in moderate yields. Photolysis of **1** in the presence of *cis*- and *trans*-1-chloropropene proceeded with high stereospecificity to give *cis*- and *trans*-1-(chlorodisilanyl)propene, respectively. Irradiation of **1** in the presence of ethyl vinyl ether afforded 1-methoxy-1-phenyl-1-vinyltrimethyldisilane after methanolysis of the photolysis product. Similar irradiation of **1** in the presence of ethyl vinyl ether, followed by treatment with hydrogen chloride, gave 1-chloro-1-(1′-ethoxyethyl)-1-phenyltrimethyldisilane and 1-chloro-1-(2′-ethoxyethyl)-1-phenyltrimethyldisilane. Irradiation of **1** with *cis*- and *trans*-1-methoxy-1-hexene, followed by ethanolysis, produced the corresponding *cis*- and *trans*-1-(ethoxydisilanyl)-1-hexene with high stereospecificity. Irradiation of **1** with vinyl acetate gave directly 1-acetoxy-1-phenyl-1-vinyltrimethyldisilane.

Introduction

In recent years, considerable attention has been devoted to investigations of silylene intermediates, and many papers that deal with addition of silylenes to carbon–carbon multiple bonds have been reported.[1-9] We have shown that trimethylsilylphenylsilylene generated by photolysis of tris(trimethylsilyl)phenylsilane adds readily to many alkenes[7,10] and alkynes[11] to give the silacyclo-

(1) Atwell, W. H.; Weyenberg, D. R. *Angew. Chem. Int. Ed. Engl.* **1969**, *8*, 469-534.

0002-7863/81/1503-4170$01.25/0